SOIL SALINITY MONITORING UNDER DIFFERENT IRRIGATION TYPES, IN SINNURIS DISTRICT, FAYOUM GOVERNORATE, EGYPT

Mahmoud M. Ali[1], Ali G. Mahmoud [2]

ABSTRACT

Soil salinity is one of the main factors limiting crop production in arid and semi-arid regions of the planet. Therefore, mapping and monitoring salinity concentrations is essential for land and water resources management and consequently for the improvement of agricultural production. The current study utilized the geostatistical Kriging method for soil data interpolation to generate soil salinity maps. In order to assess and monitor salinity changes in the study area under different irrigation types, the soil samples collected in 2018 and the soil salinity data available for 2009 were used. The results showed significant improvements in soil salinity levels, as the area of none saline soils (< 2 dS m^{-1}) increased from 1.3 ha in 2009 to 9119 ha in 2018. These impressive results could be related to the construction of sub-surface drainage systems that started in 2007, consequently, demonstrate the effectiveness of water management policies in Sinnuris District. Moreover, soil salinity values showed a negative correlation with the elevation data, which could explain the increasing salinity levels around the Lake Qarun due to the shallow saline water table and the low efficiency of the drainage system.

Keywords: *Irrigation; Soil Salinity Monitoring; Sinnuris District; Fayoum; Egypt*

INTRODUCTION

Soil salinity is considered one of the major limiting factors to crop production in arid and semi-arid regions. Besides, salinization and alkalinization are the most common soil degradation processes in such regions. These regions are under enormous pressure to provide the required food and fiber (Farifteha et al., 2006, Tripathi et al., 2015, Gorji et al., 2015).

[1] **Agriculture Engineering Department, Faculty of Agriculture, Fayoum University, Fayoum, Egypt.**

[2] **Soil and Water Department, Faculty of Agriculture, Fayoum University, Fayoum, Egypt.**

Under the conditions of current water regimes and inappropriate natural drainage systems, there is a real hazard of salt accumulation in land. Basically, this is due to the application of water containing salts, weathering both primary and secondary minerals in land, organic matter decay, and shallow and/or instability of water table (Daeia et al., 2009, Poshtmasari et al., 2012, Akramkhanov et al., 2018). On the one hand, soil salinity is, mainly, characterized as a natural process, while soil salinization is, in principle, a human-induced process (Zinck & Metternicht, 2009). On the other hand, due to the accumulation of soluble salts on or near the surface of the land, soil salinity is categorized as an in-situ form of soil degradation (Bouaziz et al., 2011), and it is counted as one of the seven main reasons to desertification (Kassas, 1987).

Mapping of the soil salinity and its variation is an essential input for the evaluation of the extent of salt build-up and thusly to propose appropriate site-specific management practices to improve the agricultural production (Kilic & Kilic, 2007). The variability of soil salinity is affected by parent material, soil type, and landscape position (Aldabaa et al., 2015). As soil salinization processes may occur at local and regional scales (Castrignano et al., 2008), Zinck & Metternicht (2009) reported several approaches developed to monitor such processes in different contexts, while case studies that use and integrate the full data are scarce. These approaches are as the following:

1. Comparing historical soil salinity maps.
2. Coping with salinity change uncertainties.
3. Incorporating contextual landscape information.
4. Recycling ancillary data in GIS context.
5. Incorporating geophysical data.
6. Integrating soil salinity and hydrology.

Geographic information system (GIS) and remote sensing (RS) technologies introduce new tools for quick field data collection and enrichment of data processing (Donia, 2009). Because the spatial distribution of soil salinity is an important source for understanding the impact of soil and water resources management in fields with different climates, thus, several statistical methods have been studied and developed, i.e. regression models, local interpolators like the deterministic method of

the inverse distance weighting (IDW), thin plate splines, and geostatistical techniques such as Kriging (Nezami & Alipour, 2012).

An experimental variogram is a plot representing the changes of one half the squared differences between the sampled values (semi-variance) with respect to the distance between point-pairs (Hengl, 2009). The general equation for computing the experimental variogram by method of moments is:

$$\hat{\gamma}(\mathrm{h}) = \frac{1}{2m(\mathrm{h})} \sum_{i=1}^{m(\mathrm{h})} \{z(\mathrm{x}_i) - z(\mathrm{x}_i + \mathrm{h})\}^2$$

Where $z(x_i)$ and $z(x_i + h)$ are the observed values of the variable z at sites x_i and $x_i + h$, and m(h) is the number of paired comparisons at a certain lag (h). Changing the lag value, h, will result in an ordered set of semi-variances (Oliver & Webster, 2015).

After calculating the experimental variogram, it can be fitted using some of the theoretical variogram models, i.e. exponential (Kaula, 1959), Gaussian (Moritz, 1972), and Stable (Wackernagel, 2003), etc. The variograms are commonly fitted by an iterative reweighted least squares estimation, where usually, the weights are determined based on the point pairs' count or based on the distance (Hengl, 2009). Thus, solving an interpolation problem can be achieved via two steps: (1) computing the experimental (empirical) variogram that well-approximate the regional variogram (2) fit this empirical variogram with a theoretical model (Chilès & Delfiner, 2012).

Our study utilized Kriging technique for the generation of soil salinity maps at two sampling epochs. Then, the obtained maps were, in depth, analyzed to assess and monitor soil salinity changes in the study area. In addition, the correlation between topography levels and soil salinity values was thoroughly investigated.

MATERIALS AND METHODS

Monitoring of soil salinity changes from 2009 to 2018 requires the integration of two different data sources. The former is the dataset of 2009, which has been conducted in 2009 to study the soil salinity levels in Sinnuris District (Mohammed, 2011). The latter is the 2018 dataset, where a fieldwork has been carried out during the winter season to collect soil

samples. Finally, the geostatistical analysis of the soil salinity datasets was performed in order to generate the salinity maps for further analyses.

Study area

Fayoum Governorate covers a circular depression in the Eocene limestone plateau at the Northern part of the Egyptian Western Desert. It is located about 90 Km Southwest to Cairo, between latitudes 29˚ 02' N and 29˚ 35' N and longitudes 30˚ 23' E and 31˚ 5' E, with a total area of about 6000 km^2 (Ali & Abdel Kawy, 2013). It is characterized by a hot dry summer with scanty winter rainfall and bright sunshine throughout the whole year. Its average temperature is 22° C, and the average annual precipitation is 7.2 mm/year, while the average rate of evaporation varies from 1.9 mm/day in January to 7.3 mm/day in June (Ali & Abdel Kawy, 2013, Abd-Elmabod et al., 2012). Fayoum governorate has a special irrigation system because of its topographic characteristics. In general, the land surface slopes regularly from South to North towards Lake Qarun with an average slope of 2 m/km. Thus, most of the governorate's land (93%) are being irrigated using direct gravity irrigation. On the other hand, the agricultural drainage water flows from South to North and finally gets discharged into both Qarun and Wadi Al Rayan Lakes (Donia, 2009).

Sinnuris District (Figure 1) represents the areas most affected by soil salinization in Fayoum, which was selected as our case study. It is located in the North part of Fayoum between latitudes 29˚ 20' N and 29˚ 30' N and longitudes 30˚ 43' E and 30˚ 56' E, and it has borders with the Southern and Eastern shores of Lake Qarun. In 2007, the execution of a sub-surface drainage system has been started in order to improve the drainage conditions on Sinnuris District and consequently the soil quality.

Fieldwork

As a pre-fieldwork step, three topographic maps (scale 1:50000) were georeferenced and used to delineate Sinnuris District boundaries with help of ArcGIS (coordinate system: UTM, WGS84, zone 36). Then, a grid of 2 x 2 km was generated to design the sampling locations (Figure 1). On the other hand, a mask of the residential areas (Figure 1) was created with the aid of topographic maps and a recent Landsat 8 image. This mask was used over both the 2009 and 2018 salinity maps in order to exclude the residential areas from the calculations. In addition, the georeferenced

topographic maps were used to digitize the contour lines and spot heights in order to generate a digital elevation model (DEM) for the study area.

The fieldwork was carried out during the period of January to February 2018. The predesigned sampling locations were reached using a global positioning system (GPS). Moreover, the defined grid points were exported to a valid keyhole markup language (KML) layer for Google Earth in order to be overlaid with the corresponding high-resolution imageries, which facilitates the navigation through the study area. For each sampling site, two disturbed samples were collected; the first sample was obtained from the surface layer to a depth of 20 cm while the second one that represents the sub-surface layer was collected at a depth of 20 to 40 cm, with a total of 120 soil samples from 60 different sites.

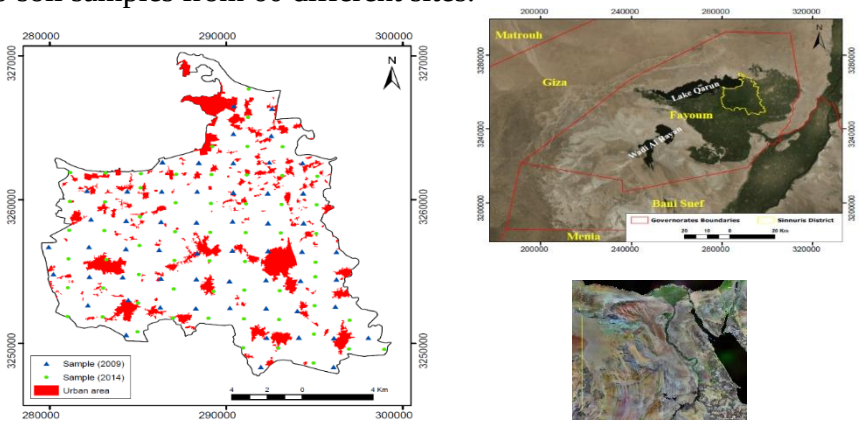

Fig. 1: Location of the study area and soil samples (2009 and 2018).

Laboratory analysis

The collected soil samples were air-dried, gently grinded, and the gradation process was performed using the 2 mm sieve to separate the fine earth fraction for preparing soil paste. Then, the measurement of the electrical conductivity of the saturated-paste extract (ECe) was fulfilled using the conductivity meter (Page et al., 1982). The measured values were stored in the attribute table of the point-map.

GIS applications

GIS functionalities were utilized to explore the data and consequently to generate the spatially distributed soil salinity maps for the two sampling epochs so that the one can evaluate the changes of soil salinity levels. Soil

salinity maps were generated using the Kriging technique that was chosen and utilized for the interpolation of the ECe values. For soil salinity datasets, different theoretical variogram models were tested and mutually compared one another in order to choose the best fitting model. Moreover, the Log-transformation was an essential pre-processing step for the non-normally distributed data.

In order to evaluate and monitor the variability of the soil salinity levels, the interpolated maps (2009 and 2018) were converted to raster (excluding the residential areas) then classified into 5 classes: non-saline (0-2 dS m^{-1}), slightly saline (2-4 dS m^{-1}), moderately saline (4-8 dS m^{-1}), strongly saline (8-16 dS m^{-1}), very strongly saline ($\geq$16 dS m^{-1}) (Soil Survey Division Staff, 1993). Finally, the classified maps were inter-compared to determine the changes in the area of each class.

RESULTS AND DISCUSSIONS

Data statistics

On the one hand, the detailed data analyses indicated that raw ECe values of the two datasets of 2009 and 2018 are not normally distributed showing high kurtosis and skewness values. Therefore, the Log-transformation, converting the skewed distribution into normal distribution, was applied before applying the Kriging analysis, which resulted in reduced skewness and kurtosis values. The graphical histograms enabled to visually test the normality of the dataset in addition to the mean and median values. The statistics of the raw and log-transformed ECe data are briefed in Table 1.

Variogram and soil salinity

Different variogram models were tested, and the least squares estimated parameters (see, Tables 2) of the different fitting theoretical models were then compared in order to select the best fitting model. As shown in Table 2, the Gaussian and Stable models have the lowest mean values of -2.282 and -0.571 and the lowest root-mean-square standardized (RMSS) values of 3.023 and 1.504 for the surface and sub-surface layers, respectively, which means that they perform better than other models to represent the spatial distribution of the ECe values for the year 2009. On the other hand, the exponential model was the best model in case of the ECe data of 2018 having the lowest mean values of -0.948 and -0.467 and the lowest RMSS of 1.756 and 1.148 for the surface and sub-surface layers, respectively

(Table 2). According to Shi et al. (2005), the Nugget/Sill ratio is an indicator to define the degree of spatial autocorrelation of the data. Although, the exponential model has a ratio lower than 25 for the 2009 ECe data (surface and sub-surface layers) reflecting a high spatial autocorrelation, it captured the high autocorrelation only for the sub-surface layer of the 2018 ECe data with a value of 8.07 (Table 2).

Table 1. Summary of the statistics of the original ECe (dS m-1) and log-transformed ECe data.

Year	Data type	Depth (cm)	Minimum	Maximum	Mean	Standard deviation	Skewness	Kurtosis	Median
2009	Raw Data	0 - 20	1.140	160.62	9.567	22.147	6.050	40.638	4.79
		20 - 40	0.880	52.73	6.316	7.927	4.254	23.374	4.325
	Log-transformed	0 - 20	0.131	5.08	1.707	0.795	1.733	8.418	1.567
		20 - 40	-0.127	3.97	1.514	0.717	0.975	4.890	1.464
2014	Raw Data	0 - 20	0.135	101.00	4.918	13.296	6.539	47.186	1.885
		20 - 40	0.240	67.90	4.440	9.333	5.707	37.813	2.310
	Log-transformed	0 - 20	-2.003	4.62	0.791	1.071	0.657	5.027	0.634
		20 - 40	-1.427	4.22	0.831	1.029	0.503	4.066	0.837

Table 2. Summary of the different variogram models used to fit the Log-transformed ECe values of the surface and sub-surface layers (2009 and 2018).

	Circular		Spherical		Exponential		Gaussian		Stable	
	surface	sub-surface	surface	sub-surface	surface	sub-surface	surface	sub-surface	surface	sub-surface
2009										
Samples	56	56	56	56	56	56	56	56	56	56
Mean	-2.306	-0.608	-2.328	-0.626	-2.366	-0.659	-2.282	-0.571	-2.282	-0.571
RMS	21.655	7.225	21.687	7.245	21.768	7.302	21.600	7.166	21.6	7.166
MS	-0.323	-0.111	-0.339	0.122	-0.368	-0.154	-0.308	-0.087	-0.308	-0.087
RMSS	3.049	1.566	3.119	1.605	3.215	1.697	3.023	1.504	3.023	1.504
ASE	5.789	3.971	5.745	3.939	5.676	3.900	5.834	4.012	5.834	4.012
Lag Size	2138.8	2138.8	2138.8	2138.8	2138.8	2138.8	2138.8	2138.8	2138.8	2138.8
Nugget	0.298	0.232	0.283	0.221	0.178	0.137	0.380	0.300	0.380	0.300
Partial Sill	0.578	0.489	0.547	0.460	0.632	0.524	0.519	0.441	0.519	0.441
Nugget/Sill	34.02	32.18	34.10	32.45	21.98	20.73	42.27	40.49	42.27	40.49
2014										
Samples	60	60	60	60	60	60	60	60	60	60
Mean	-1.021	-0.581	-1.007	-0.571	-0.948	-0.467	-1.026	-0.673	-1.026	-0.673
RMS	12.750	8.649	12.750	8.633	12.742	8.481	12.757	8.685	12.757	8.685
MS	-0.164	-0.042	-0.168	-0.039	-0.161	-0.025	-0.173	-0.045	-0.173	-0.045
RMSS	1.770	1.230	1.774	1.220	1.756	1.148	1.775	1.261	1.775	1.261
ASE	5.342	4.572	5.388	4.588	5.545	4.869	5.349	4.443	5.349	4.443
Lag Size	1250.4	1002.9	1287.2	1179.9	1978.0	929.9	974.2	733.0	974.2	733.0
Nugget	0.616	0.395	0.591	0.382	0.525	0.090	0.696	0.489	0.696	0.489
Partial Sill	0.664	0.736	0.670	0.774	0.836	1.025	0.520	0.511	0.520	0.511
Nugget/Sill	48.13	34.92	46.87	33.04	38.57	8.07	57.24	48.90	57.24	48.90

RMS: root mean square MS: mean standardized RMSS: root-mean-square standardized ASE: average standard error

The resulted soil salinity maps of 2009 using the Gaussian model were compared to the measured data, it was found that the area around the Lake Qarun is underestimated. Therefore, the exponential model was selected to fit all the salinity variograms (2009 and 2018) as shown in Figure 2, and the obtained soil salinity maps are shown Figure 3.

Soil salinity monitoring

It is obvious from the developed soil salinity maps that the soil salinity levels have significantly decreased in 2018 that can be attributed to the construction of the new sub-surface drainage system in the study area, which started in 2007. Nowadays, most of the study area is served by this system except a small area located in the western-north part.

As illustrated in Table 3, the largest area in 2009 of about 13336 ha corresponds to the slightly saline class (4-8 dS m^{-1}) of the surface layer. This area is sequentially bounded to the North by elongated areas that belong to the strong and very strong salinity classes. Nevertheless, these areas are in relative vicinity to Lake Qarun that is characterized with a shallow saline water table and poor drainage conditions leading to a noticeable rise in soil salinity levels.

On the other hand, for the surface layer in 2018, the largest area coincides to the non-saline soils with a total area of 9119 ha (in comparison to 1.3 ha in 2009), which represents a significant improvement in soil salinity levels where about 9118 ha transformed to non-saline class from higher salinity ones. The slightly saline soils come in the second place with area of 7898 ha. As for the higher salinity classes, the area of the surface layer of each class in 2018 has significantly decreased in comparison to these in 2009 showing a significant improvement in soil salinity in the study area. While the areas that had the highest salinity values were still those adjacent to the Lake Qarun. Figure 4 shows the areas (in percentage with respect to the total area) of the different soil salinity classes in the study area.

Figure 5 shows the spatial distribution of the variation of soil salinity levels between 2009 and 2018 for the surface and sub-surface layers. It illustrates that the western north area showed low improvements in soil salinity. This can be attributed to the deficiency of adequate and proper drainage systems, as the recently constructed system does not cover yet this region.

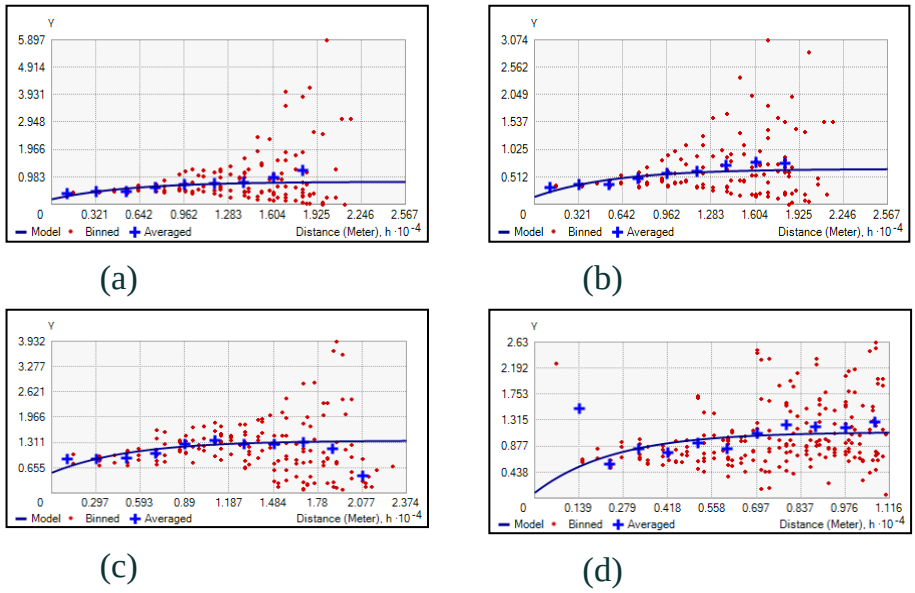

Fig. 2: Variograms of the soil salinity data fitted using the exponential model; (a) surface layer, (b) sub-surface layer for 2009, and (c) surface layer, (d) sub-surface layer for 2018.

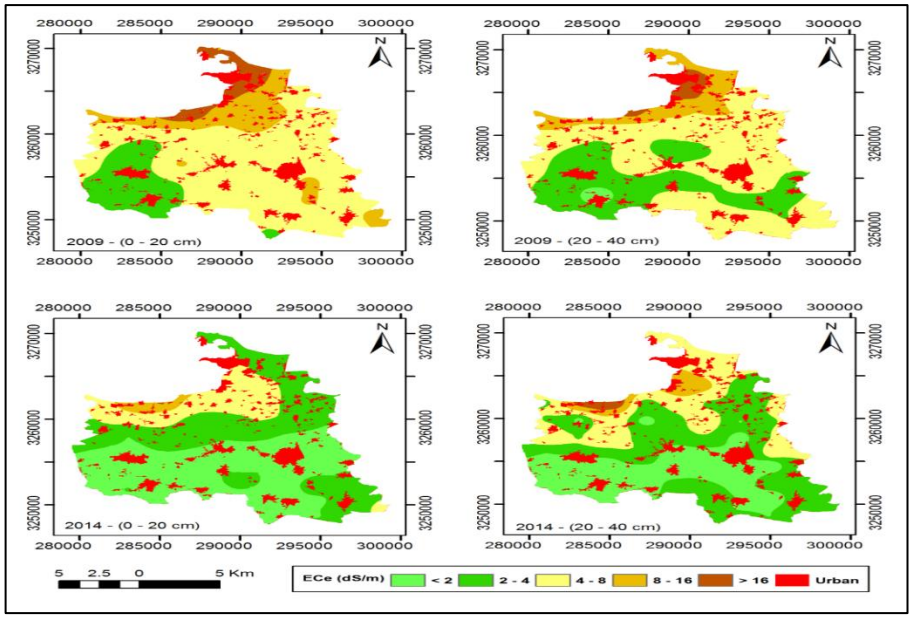

Fig. 3: The Salinity maps for the surface and sub-layers of the study area (2009 and 2018) developed using the exponential model.

Table 3. The area (in hectare) of the different Salinity classes for 2009 and 2018.

ECe (dS m^{-1})	Layer 0 – 20 cm		Layer 20 – 40 cm	
	2009	2018	2009	2018
< 2	1.28	9119.16	218.26	6211.88
2 – 4	3245.43	7898.45	6528.10	8401.42
4 – 8	13336.03	3220.37	11237.84	5056.02
8 – 16	3031.36	406.13	2252.69	777.45
> 16	1037.71	7.69	414.91	205.03

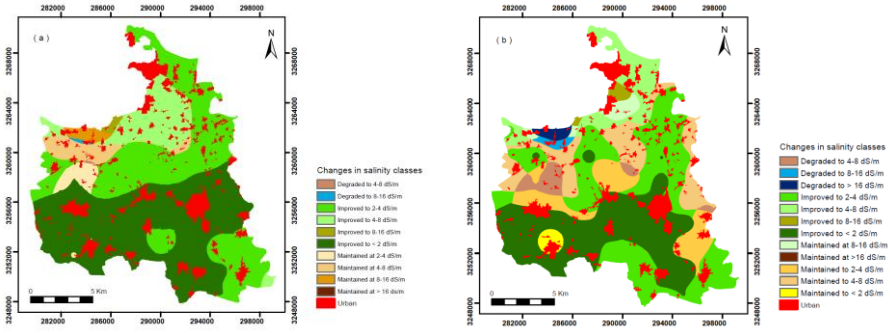

Fig. 4: The spatial distribution of the changes in soil salinity levels between 2009 and 2018 in the study area; a) surface layer, and b) sub-surface layer.

Topography and soil salinity changes

The DEM constructed for our study area has a spatial resolution of 5 m (Figure 6). The altitude ranges from 22 m close to the southern border and decreases upwards reaching -44 m at the Coast of Lake Qarun at the north border of the study area. Table 4 reports the correlation matrix between the DEM and soil salinity maps of 2009 and 2018 for surface and sub-surface layers.

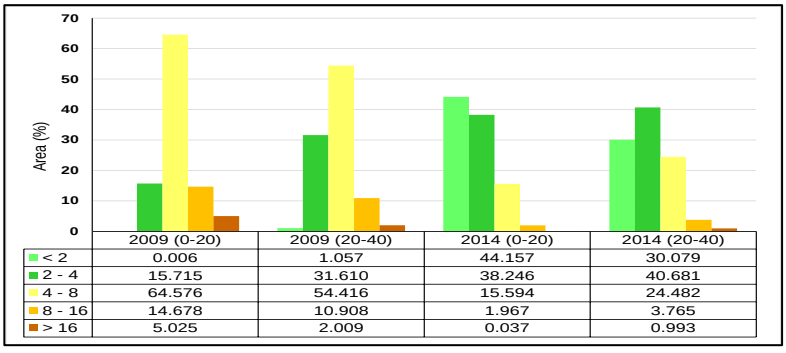

	2009 (0-20)	2009 (20-40)	2014 (0-20)	2014 (20-40)
< 2	0.006	1.057	44.157	30.079
2 - 4	15.715	31.610	38.246	40.681
4 - 8	64.576	54.416	15.594	24.482
8 - 16	14.678	10.908	1.967	3.765
> 16	5.025	2.009	0.037	0.993

Fig. 5: The area (in percent) of the different soil salinity classes within the study area.

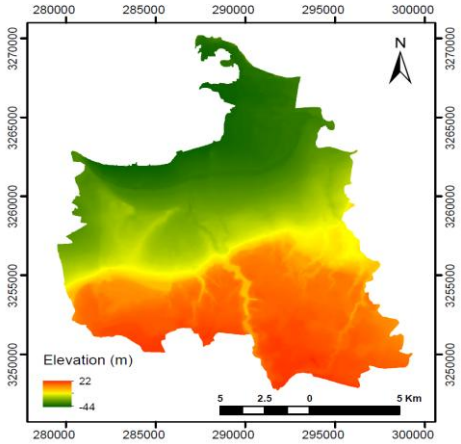

Fig. 6: The 5-m spatial resolution digital elevation model of the study area.

Table 4. The correlation matrix between DEM and soil salinity levels of 2009 and 2018.

		DEM	**Soil Salinity (2009)**		**Soil Salinity (2018)**	
			(0 – 20)	**(20 – 40)**	**(0 – 20)**	**(20 – 40)**
DEM		1				
Soil Salinity (2009)	(0 – 20)	-0.74	1			
	(20 – 40)	-0.61	0.750	1		
Soil Salinity (2018)	(0 – 20)	-0.68	0.002	0.61	1	
	(20 – 40)	-0.58	0.180	0.53	0.86	1

As shown in table 4, there is, in general, a negative correlation between the elevation and soil salinity in different layers with a minimum value of -0.74 for the surface layer of 2009 dataset. This could explain the increasing salinity levels around the Lake Qarun due to the shallow saline water table and the low efficiency of the drainage system, as well as the effects of the high salinity of Lake Qarun's water. On the other hand, the correlation between the surface and sub-surface layers of each dataset is higher than that between the 2009 and 2018 datasets. The correlation between the surface layer in 2009 and the two layers of 2018 revealed the lowest correlation values. This could be explained as the improvement of the soil salinity level has occurred on irregular manners regardless to the initial salinity class in 2009. While, the negative correlation values between topography and the soil salinity levels in 2009 and 2018 reflect the significant effect of such a local topography.

CONCLUSION

The Kriging technique was selected and utilized in order to produce the soil salinity maps for Sinnuris District for years 2009 and 2018. Different variogram models have been explicitly studied to fit the empirical variogram of the soil salinity levels, where the exponential model was the best fitting model. Furthermore, the soil salinity levels increased in the northern part with the decreasing distance to the Lake Qarun. This could be justified by the high effects of the topography, as the probability of having a shallow and saline ground water table increases as impact to the existence of Lake Qarun. Furthermore, a detailed comparison between the resulted salinity maps was performed showing significant improvements in soil salinity levels between the two sampling epochs, with an increase of the area of non-saline soils (< 2 dS m^{-1}) from 1.3 ha in 2009, to 9119 ha in 2018. Such Improvements could be partly linked to the construction of a new sub-surface drainage system, which started in 2007, and the effectiveness of the water management policies in Sinnuris District.

REFERENCES

ABD-ELMABOD, S. K., ABDELMAGEED, T. A., ALÍ, R. R., ANAYA ROMERO, M., JORDÁN, A., MARTÍNEZ ZAVALA, L., MUÑOZ ROJAS, M. & ROSA, D. D. L. 2012. Evaluating soil degradation under different scenarios of agricultural land management in Mediterranean region. Nature and Science, 10, 103-116.

AKRAMKHANOV, A., BRUS, D. J. & WALVOORT, D. J. J. 2018. Geostatistical monitoring of soil salinity in Uzbekistan by repeated EMI surveys. Geoderma, 213, 600-607.

ALDABAA, A. A. A., WEINDORF, D. C., CHAKRABORTY, S., SHARMA, A. & LI, B. 2015. Combination of proximal and remote sensing methods for rapid soil salinity quantification. Geoderma, 239-240, 34-46.

ALI, R. R. & ABDEL KAWY, W. A. M. 2013. Land degradation risk assessment of El Fayoum depression, Egypt. Arabian Journal of Geosciences, 6, 2767-2776.

BOUAZIZ, M., MATSCHULLAT, J. & GLOAGUEN, R. 2011. Improved remote sensing detection of soil salinity from a semi-arid climate in Northeast Brazil. Comptes Rendus Geoscience, 343, 795–803.

CASTRIGNANO, A., BUTTAFUOCO, G. & PUDDU, R. 2008. Multi-scale assessment of the risk of soil salinization in an area of south-eastern Sardinia (Italy). Precis Agric, 9, 17–31.

CHILÈS, J. P. & DELFINER, P. 2012. Geostatistics: Modeling Spatial Uncertainty, Wiley.

CRESSIE, C. 1990. The origins of kriging. Mathematical Geology, 22, 239-252.

DAEIA, G., ARDEKANIA, M. R., REJALIC, F., TEIMURIB, S. & MIRANSAR, M. 2009. Alleviation of salinity stress on wheat yield, yield components, and nutrient uptake using arbuscular mycorrhizal fungi under field conditions. Journal of Plant Physiology, 166, 617-625.

DONIA, N. 2009. Application of remotely sensed imagery to watershed analysis; A case study of Lake Karoun catchment, Egypt. Thirteenth International Water Technology Conference. IWTC: Hurghada, Egypt.

ELBASIOUNY, H., ABOWALY, M., ABU_ALKHEIR, A. & GAD, A. A. 2018. Spatial variation of soil carbon and nitrogen pools by using ordinary Kriging method in an area of north Nile Delta, Egypt. Catena, 113, 70-78.

HENGL, T. 2009. A Practical Guide to Geostatistical Mapping, BPR Publishers.

KASSAS, M. 1987. Seven paths to desertification. Desertification Control Bulletin, 15, 24–26.

KAULA, W. M. 1959. Statistical and harmonic analysis of gravity. Journal of Geophysical Research, 2401-2421.

KILIC, K. & KILIC, S. 2007. Spatial variability of salinity and alkalinity of a field having salination risk in semi-arid climate in northern Turkey. Environ Monit Assess, 127, 55-65.

MOHAMMED, A. H. M. 2011. Studies on Ground Water of some Soils in Fayoum Governorate Using GIS. M.Sc. M.Sc., Fayoum University.

MORITZ, H. 1972. Advanced least-squares estimation. The Ohio State University, Department of Geodetic Science.

NEZAMI, M. T. & ALIPOUR, Z. T. 2012. Preparing of the soil salinity map using geostatistics method in the Qazvin Plain. Journal of Soil Science and Environmental Management, 3, 36-41.

OLIVER, M. A. & WEBSTER, R. 2015. Basic Steps in Geostatistics: The Variogram and Kriging, Springer International Publishing.

POSHTMASARI, H. K., SARVESTANI, Z. T., KAMKAR, B., SHATAEI, S. & SADEGHI, S. 2012. Comparison of interpolation methods for estimating pH and EC in agricultural fields of Golestan province (north of Iran). International Journal of Agriculture and Crop Sciences, 4, 157-167.

WACKERNAGEL, H. 2003. Multivariate Geostatistics: An Introduction with Applications, Springer Berlin Heidelberg.

ZINCK, J. A. & METTERNICHT, G. 2009. Soil Salinity and Salinization Hazard. In: METTERNICHT, G. & ZINCK, J. A. (eds.) Remote sensing of soil salinization: impact on land management. Taylor & Francis Group.

الملخص العربي

رصد ملوحة التربة تحت تأثير أنواع الري المختلفة، بمركز سنورس، محافظة الفيوم، مصر

محمود محمد علي [١] – علي جابر محمود [٢]

تعد ملوحة التربة أحد أهم العوامل التي تحد من إنتاج المحاصيل في المناطق الجافة وشبه الجافة. لذلك، يعد متابعة ورصد الملوحة ضروريًا لإدارة موارد الأراضي والمياه وبالتالي لتحسين الإنتاج الزراعي. استخدمت الدراسة الحالية طريقة كريجنج الاحصائية لاستيفاء بيانات التربة وترسيم خرائط ملوحة التربة. ومن أجل تقييم ورصد التغيرات في الملوحة في منطقة الدراسة - تبعاً لنظم الري المختلفة - تم استخدام عينات التربة التي تم جمعها في عام ٨٢٠١ وبيانات ملوحة التربة المتاحة لعام ٢٠٠٩. أظهرت النتائج تحسنا ملحوظا في مستويات ملوحة التربة، حيث زادت مساحة التربة غير المالحة (<2 dS m-1) من ١,٣ هكتار في عام ٢٠٠٩ إلى ٩١١٩ هكتار في عام 2018. ويمكن أن تكون هذه النتائج مرتبطة بتشكيل سطح تحت سطح الأرض وشبكات الصرف الصحي التي بدأت في عام ٢٠٠٧، وبالتالي، تظهر فعالية سياسات إدارة المياه في سنورس. علاوة على ذلك، أظهرت قيم ملوحة التربة وجود علاقة سلبية مع بيانات الارتفاع، والتي يمكن أن تفسر زيادة مستويات الملوحة حول بحيرة قارون بسبب منسوب المياه المالحة الضحلة وانخفاض كفاءة نظام الصرف.

الكلمات المفتاحية:
الري؛ رصد ملوحة التربة. منطقة سنورس الفيوم. مصر.

[١] قسم الهندسة الزراعية، كلية الزراعة، جامعة الفيوم، الفيوم، مصر.
[٢] قسم التربة والمياه، كلية الزراعة، جامعة الفيوم، الفيوم، مصر.